Int. J. Environ. Sci. Technol. (2015) 12:4017–4024
DOI 10.1007/s13762-015-0832-z

ORIGINAL PAPER

Adsorption of chromium(VI) onto electrochemically obtained magnetite nanoparticles

L. J. Martínez[1] · A. Muñoz-Bonilla[1] · E. Mazario[1] · F. J. Recio[2] · F. J. Palomares[3] · P. Herrasti[1]

Received: 18 December 2014 / Revised: 20 March 2015 / Accepted: 2 June 2015 / Published online: 12 June 2015

Abstract Well-dispersed magnetite nanoparticles of different sizes between 15 and 43 nm were synthesized by an electrochemical method in a controlled manner by simply changing the synthesis temperature. These nanoparticles were used as a reusable adsorbent to remove Cr(VI) from aqueous solution. The recovery efficiency was found to be highly dependent on environmental parameters, such as temperature and pH. In addition, it was demonstrated that the initial concentrations of both Cr(VI) and magnetite nanoparticles strongly influence the removal capability of these nanomaterials. Remarkably, the nanoparticle size has a key role on the Cr(VI) adsorption efficiency, which gradually increases as the diameter decreases due to the augmentation of the surface area. The low aggregation in the case of small particles that results from the low magnetization saturation values also contributes to the enhancement of the surface area available for Cr(VI) adsorption. In contrast, nanoparticles with larger sizes are more easily manipulated by a magnet, and the efficiency is largely maintained after five cycles. The adsorption process fits the Langmuir isotherm model well, and the reaction was found to follow a pseudo-second-order rate.

✉ P. Herrasti
pilar.herrasti@uam.es

[1] Departamento de Química Física Aplicada, Facultad de Ciencias, Universidad Autónoma de Madrid, 28049 Madrid, Spain

[2] Departamento de Química de los Materiales, Facultad de Química y Biología, Universidad de Santiago de Chile, Casilla 40, Correo 33, Santiago, Chile

[3] Instituto de Ciencia de Materiales de Madrid, ICMM-CSIC, 28049 Cantoblanco, Madrid, Spain

Keywords Magnetite nanoparticles · Cr(VI) removal · Adsorption · Remediation

Introduction

Industrial activities generate different types of waste that cause pollution in soil, water and air as a consequence of either ignorance or mismanagement. This can permanently affect the environment if the discharges are persistent or severe enough to be unable to be assimilated. A clear example is the pollution produced by heavy metal discharges to the environment. Although some heavy metals are essential for life, others are very toxic, even at low concentrations. Among heavy metals, chromium is generally considered to be very harmful to health, especially Cr(VI). Indeed, the United States Environmental Protection Agency (EPA) fixed the maximum contaminant level for chromium in drinking water at 0.1 mg/L. Several processes have been developed to eliminate the chromium present in industrial wastewater (Singh and Prasad 2015). The most commonly used methods to reduce the concentration of Cr(VI) in aqueous solutions are ion exchange, polymer resins, coagulation–flocculation, activated carbon adsorption and the reduction/chemical precipitation/sedimentation process (Boddu et al. 2003; Hu et al. 2004; Patterson et al. 1997). Although the last method is probably the most commonly employed, it is very inefficient because a large amount of sludge is produced and the chromium cannot be recovered from the precipitate, making this strategy very expensive (Leyva Ramos et al. 1994). On the other hand, adsorption is considered to be an efficient method for removing heavy metals from wastewater (Aggarwal et al. 1999; Selvi et al. 2001).

Various adsorbent materials have been tested to remove Cr(VI) from aqueous solution. These materials include

activated carbon, activated alumina, natural zeolites and various biosorbents (Faghihian and Bowman 2005; Khezami and Capart 2005; Mor et al. 2007). However, these adsorbents present a common problem, the need for a second separation process from solution, which increases operating costs.

Recently, the use of magnetic materials has attracted increasing interest because they allow for the easy separation of the material from the working environment by using a magnet (Crane et al. 2011). Unfortunately, bulk magnetic materials have a low surface area, which means that the adsorption process is not realistic for the treatment of waste-containing heavy metals, in this particular case, Cr(VI). From this point of view, increasing the active surface area is necessary to use these magnetic materials as adsorbents. To augment the active surface area, the crystal size of the magnetic material should be reduced to the nanoscale. Recent studies have shown that magnetite nanoparticles can efficiently adsorb heavy metals, including arsenic, lead, copper and chromium (Hu et al. 2006, 2007; Liu et al. 2012; Vunain et al. 2013).

The current study investigates the Cr(VI) adsorption ability of magnetite nanoparticles obtained via an electrochemical route. The influence of parameters such as the pH, temperature and size of the nanoparticles on the adsorption capability has been studied in detail, as well as the reusability of these nanoparticles as adsorbents. The type of adsorption isotherm and the kinetics of the process are also presented.

Materials and methods

Electrochemical synthesis

Magnetite nanoparticles (Nps) of different sizes were synthesized using an electrochemical method developed by Cabrera et al. (2008). Briefly, foils of iron (99.5 %, Goodfellow) were used as the anode and cathode, with areas of 2 and 4 cm^2, respectively, and were immersed in an electrolyte solution of tetrabutyl ammonium bromide (0.04 M, Aldrich), which also acts as a surfactant to avoid agglomeration. In all cases, a constant current of 50 mA/cm^2 was applied using an AMEL model 549 potentiostat/galvanostat for 30 min. Constant stirring was maintained at 1100 rpm, and the synthesis temperature was varied from 5 to 60 °C to obtain nanoparticles of various sizes.

Nanoparticle characterization

The crystalline phase and the crystal size of the synthetized nanoparticles were studied by X-ray diffraction using a X'Pert PANalytical diffractometer with Cu–Kα radiation. The diffraction patterns were analysed using the Fullprof suite (Roisnel and Rodriguez-Carvajal 2000) based on the Rietveld method. Transmission electron micrographs were acquired on a JEOL JEM 1010 operating at an acceleration voltage of 100 kV. Samples were prepared by placing a small droplet of the colloidal solution on a copper grid with an amorphous carbon support film and allowing it to dry overnight.

The Z potential of the colloids was measured using a Malvern Z sizer nano DLS instrument, and the pH was adjusted by the addition of HCl or NaOH.

X-ray photoelectron spectroscopy (XPS) experiments were performed in an ultrahigh vacuum (UHV) chamber with a base pressure of 10^{-9} mbar using a hemispherical electron energy analyser (SPECS Phoibos 150 spectrometer) and a monochromatic AlKα (1486.74 eV) X-ray source. XPS spectra were recorded at a normal emission take-off angle using an energy step of 0.1 eV and a pass energy of 20 eV, which provides an overall instrumental peak broadening of 0.55 eV (Sanchez-Garcia et al. 2009). Data processing was performed using CasaXPS software (Casa Software Ltd., Cheshire, UK).

Adsorption experiments

Chromium(VI) concentrations were measured by a Perkin Elmer model Lambda35 UV–visible spectrometer, and the samples were tested in triplicate. A calibration curve with Cr(VI) concentrations ranging from 10 to 100 mg/L was generated. A certain amount of magnetite nanoparticles (0.5–2.0 mg/mL) was added to chromium(VI) aqueous solutions of different concentrations, and the mixtures were magnetically stirred. After a desired time, the nanoparticles were easily removed from the solution using external magnetic forces. Samples were collected at different times, and the absorbance of these solutions was measured. The chromium adsorption experiments were performed at various pH values and temperatures and using four different magnetic nanoparticle sizes.

Results and discussion

Nanoparticle characterization

Different iron oxide nanoparticles were synthetized by varying the diameter to investigate the effect of the particle size and thereby the surface area for the removal of chromium from aqueous solution. The electrochemical synthetic method allows for the control of the particle size by the simple variation of the reaction temperature (Mazario et al. 2012). In particular, the experiments were carried out at 5, 20, 40 and 60 °C. First, the nanoparticles obtained at each temperature were analysed by XRD. Diffraction peaks

appeared in the patterns of all of the nanoparticles at 2θ values of 18.2°, 30.1°, 35.5°, 37.1°, 43.1°, 53.4°, 56.9° and 62.6°, corresponding to (111), (220), (311), (222), (400), (422) and (511) Bragg's reflections, respectively, and can be indexed to the spinel magnetite (Fd-3m) without further peaks corresponding to intermediates of the reaction or other impurities. The average crystallite size of the magnetite nanoparticles estimated by Rietveld shows that the diameter increases with the temperature, with sizes of 15, 23, 28 and 35 nm, for reaction temperatures of 5, 20, 40 and 60 °C, respectively. The obtained nanoparticles were further characterized by TEM, as displayed in Fig. 1. Quasi-spherical nanocrystallites are clearly observed for all the investigated temperatures. The mean diameter and the particle size distribution were estimated from the TEM images by counting at least 100 nanoparticles, showing that the NP size progressively increments as the temperature increases, in agreement with the trend measured by XRD, with values of 16, 21, 36 and 43 nm. Concomitantly, the nanoparticles tend to aggregate as the diameter increases, especially for the largest particles, which affects the chromium adsorption.

Effect of pH on the Cr(VI) recovery

pH is one of the most important parameters affecting the adsorption process because Cr(VI) is present in different ionic forms depending on the pH conditions. In principle, Cr(VI) uptake by iron oxide nanoparticles is favoured at acidic pH (Burks et al. 2014), as the predominant form in solution is the hydrogen chromate ion ($HCrO_4^-$) (Benefield 1982), while the magnetite surface becomes more positively charged and thereby facilitates the attraction of these negatively charged species. Zeta potential experiments at different pH values were carried out to corroborate the surface charge of the magnetite nanoparticles. As expected, the surface of the Fe_3O_4 Nps exhibits positive charges at acidic pH (isoelectric point at pH 6.2) due to the dominant groups that are generated at the surface, mainly Fe^{2+}, Fe^{3+} and $FeOH^+$, which attract negatively charged pollutants (Chowdhury et al. 2012). Z potential experiments on colloidal magnetite nanoparticles also show the stability of this colloid at pH values below 5, with a Z potential higher than +20 mV. Therefore, the stability of the colloid is very important to consider in determining whether this system is able to adsorb ions from solution.

Afterwards, the ability of Fe_3O_4 nanoparticles to adsorb Cr(VI) was tested by varying the contact time at pH 3.5. Figure 2 displays the results as a function of the time for NPs with a diameter of 21 nm (2 mg/mL) and an initial Cr(VI) concentration of 80 mg/L at room temperature. It is clearly observed that the adsorption rate was initially rapid because of the high number of vacant adsorption sites available on the surface, and then, a plateau was reached, indicating saturation. A similar behaviour was found for all tested concentrations, with equilibrium reached in 20 min in all of the cases. This time is comparable to the equilibrium time achieved by Hu et al. (2004) and is lower than that obtained by Chowdhury et al. (2012), who used magnetite–maghemite as the adsorbent. Subsequently, the effect of pH as well as of other parameters on the removal of Cr(VI) by the magnetite nanoparticles was studied with a contact time of 30 min to assure equilibrium. Figure 3a shows that the adsorption of Cr(VI) decreases as the pH increases, and this reduction in the removal capability is more notable at pH 4.5. Although the efficiency is higher at low pH, the magnetic nanoparticles can be partially

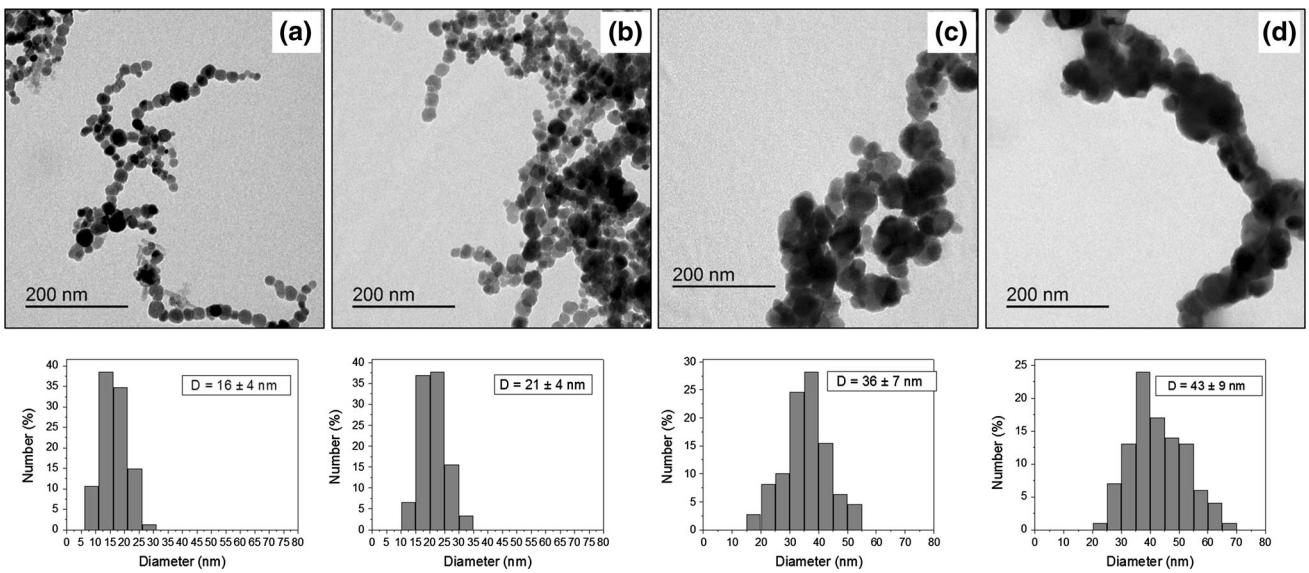

Fig. 1 TEM micrographs and particle size distributions of different magnetite nanoparticles synthetized electrochemically

dissolved at a very acidic pH, (Burks et al. 2014) even with the surfactant cover that can protect them from dissolution. As the recyclable and reusable capacity of the magnetic nanoparticles is also investigated in this work, it is important to avoid, as much as possible, the dissolution of the particles. Therefore, a relatively moderate acidic pH value of 3.5 is selected in this study, with a fairly acceptable chromium removal efficiency. At this pH, the zeta potential of the magnetic Nps is higher than +20 mV, exhibiting good colloidal stability and a suitable positive charge for attracting the negatively charged chromium species in solution through electrostatic interactions.

Effect of the temperature on the Cr(VI) recovery

The effect of temperature on the percentage of chromium removal was also investigated as a crucial factor affecting the efficiency of the process. Experiments were carried out using nanoparticles with a diameter of 21 nm as the adsorbent (2 mg/mL) at an initial chromium concentration of 80 mg/L. A contact time of 30 min and a nanoparticle concentration of 2 mg/mL were fixed for all the experiments, while the pH was set at 3.5. Figure 3b shows that the efficiency clearly increases as the temperature increases from 10 to 75 °C. This increase may be attributed to the enhancement of the Cr(VI) diffusion from the solution to the adsorbent surface when the temperature rises, probably due to the decrease in the solution viscosity and the increase in the collision frequency. Once the Cr(VI) is located on the outer nanoparticle surface, there might be electrostatic attraction occurring between the adsorbate and adsorbent (Singh et al. 1993). In addition to this effect, varying the temperature would modify the equilibrium capacity (Khezami and Capart 2005). It is noteworthy that the efficiency increases from 10 °C to reach a plateau at approximately 40 °C and subsequently sharply increases at higher temperatures. Previous studies using magnetic nanoparticles as adsorbents showed optimal temperatures between 25 and 40 °C, but higher temperatures were not further investigated in those works (Dula et al. 2014; Shahriari et al. 2014; Sharma and Srivastava 2010).

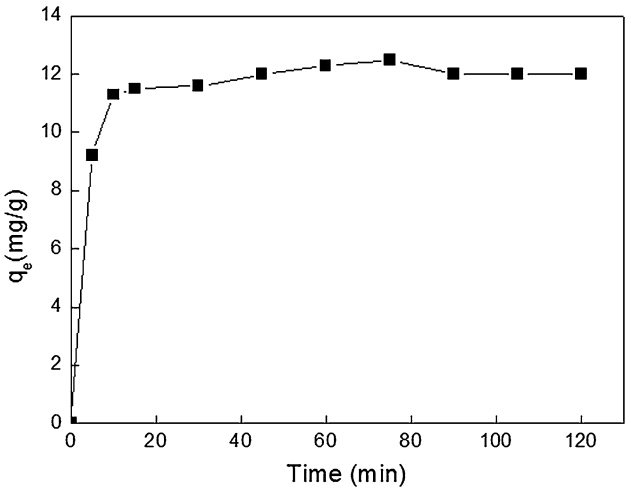

Fig. 2 Effect of contact time on the adsorption of Cr(VI) at an initial concentration of 80 mg/L at 20 °C and pH 3.5 using magnetite nanoparticles with a 21 nm diameter at a concentration of 2 mg/mL

Effect of the initial concentration of Cr(VI) and the nanoparticles on the Cr(VI) recovery

The initial concentration is also a key parameter to take into consideration, as the diffusion of the ions to the nanoparticles is governed by the concentration. Figure 3c shows the efficiency as a function of the initial concentration of Cr(VI) for magnetite nanoparticles with a diameter of 21 nm at a concentration of 2 mg/mL. It is observed that the adsorption increases when the initial concentration of Cr(VI) is higher. This is due not only to an enhancement in the diffusion but also as a result of the incrementation of the number of ions competing for the

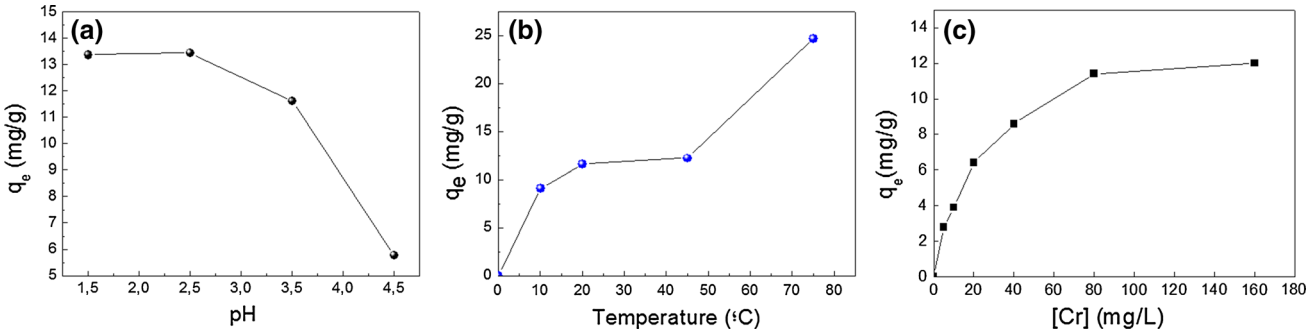

Fig. 3 **a** Effect of the initial solution pH on the chromium removal efficiency (q_e) at an initial Cr(VI) concentration of 80 mg/L and 20 °C using magnetite nanoparticles with a 21 nm diameter at a concentration of 2 mg/mL. **b** Effect of the reaction temperature on (q_e) at an initial Cr(VI) concentration of 80 mg/L and pH 3.5 using magnetite nanoparticles with a 21 nm diameter at a concentration of 2 mg/mL. **c** Effect of the initial Cr(VI) concentration on (q_e) at 20 °C and pH 3.5 using magnetite nanoparticles with a 21 nm diameter at a concentration of 2 mg/mL

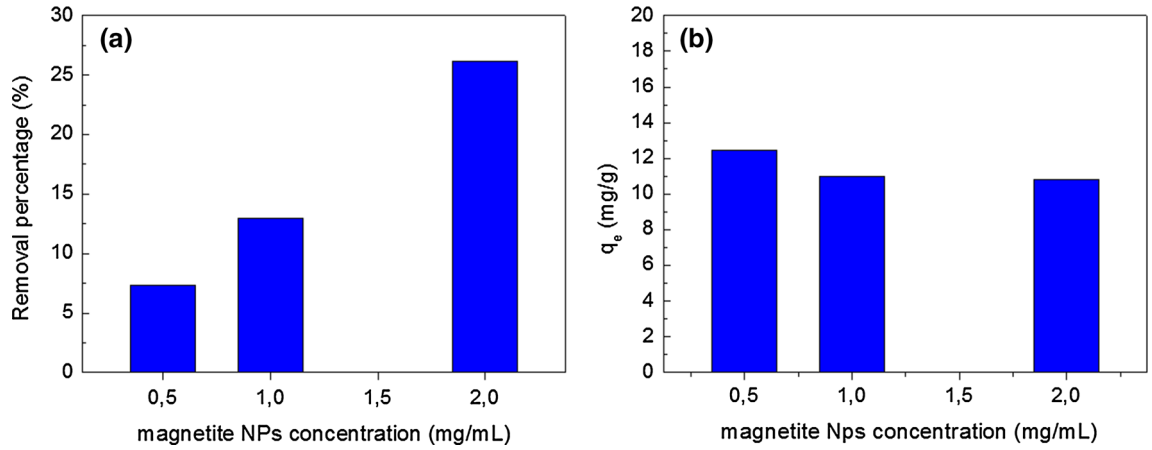

Fig. 4 Effect of the magnetite nanoparticle concentration on the adsorption of Cr(VI) at an initial Cr(VI) concentration of 80 mg/L, 20 °C and pH 3.5, using NPs with a 21 nm diameter. **a** Removal percentage (%) versus magnetite concentration and **b** efficiency (mg/g) versus magnetite concentration

available binding sites on the nanoparticle surfaces. When the concentration of Cr(VI) is low, the $[Fe_3O_4]/[Cr(VI)]$ ratio is high, and therefore, the surface of the nanoparticles is largely available for adsorption. However, when this ratio decreases, the surface can be completely covered by Cr(VI) and no additional Cr(VI) can be adsorbed. The Cr(VI) adsorption reaches a plateau at 80 mg/L, showing a saturation of binding sites at higher concentration levels.

Then, the effect of the initial amount of nanoparticles added to the chromium solution was studied. Different concentrations of magnetite nanoparticles were employed, 0.5, 1.0 and 2.0 mg/mL, fixing the initial Cr(V) concentration at 80 mg/L in each experiment. Figure 4a shows that the percentage of adsorbed Cr(VI) rises with the increment of the magnetite nanoparticles used as adsorbents. However, the removal efficiency, defined as the amount of adsorbate adsorbed per unit mass of adsorbent (q_e), does not vary significantly with the amount of magnetite nanoparticles added to the solution, as displayed in Fig. 4b. This fact indicates that in the investigated range of nanoparticle concentration, the aggregation of nanoparticles is very limited, consequently maintaining the active area for adsorption.

Effect of the nanoparticle size on the Cr(VI) recovery and regeneration of the magnetite nanoparticles

Another important factor that strongly affects the adsorption of Cr(VI) by magnetic nanoparticles is the particle size and therefore the surface area of the adsorbent. In spite of its importance, the effect of the adsorbent size has not been extensively studied until now. The electrochemical synthesis employed for the preparation of the magnetite nanoparticles allows for the easy control of the nanoparticles by simply varying the reaction temperature. The

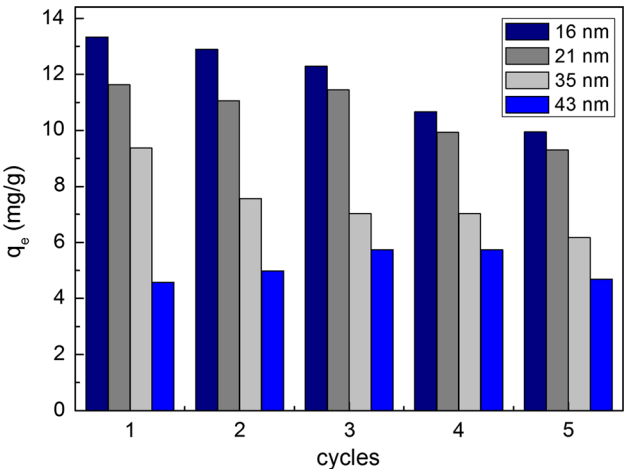

Fig. 5 Chromium removal efficiency (q_e) during five recycle experiments of magnetite nanoparticles of different sizes

diameter was varied from 16 to 43 nm (as measured by TEM) (see Fig. 5, first cycle). The recovery efficiency significantly increases when the particle size decreases to 13.3 mg/g for a NP of 16 nm, which is a relatively high value in comparison with other unsupported systems reported in the literature (Chowdhury et al. 2012; Yuan et al. 2009). This is because the surface/volume ratio increases, thus augmenting the surface available for adsorption as a result of not only the smaller particle size but also to the dispersibility of the NPs. The agglomeration of NPs is significant for nanoparticle sizes >36 nm, as demonstrated by TEM, which further reduces the surface available for Cr(VI) adsorption. The magnetization saturation generally decreases with the diameter, and therefore, the aggregation of the particles decreases, but at the same time, the manipulation and recovery of the nanoparticles by external magnetic fields could become more difficult.

A regenerative test was conducted to evaluate the reusability of electrosynthesized Fe_3O_4 NPs of different sizes. The study was carried out following the route previously proposed by Hu et al. (2006), in which the chromium-loaded magnetite NPs were incubated in a 0.01 M NaOH solution for 30 min to remove the adsorbed Cr(VI) ions before being repeatedly washed with distilled water. Then, the surface chemical composition of the samples was analysed by XPS measurements. Carbon and hydroxyl (OH) species were detected as contaminants on the surface of the samples. The overall surface composition was determined from survey spectra with regions of interest of (Fe2*p*, Cr2*p*, O1*s*, C1*s*). Figure 6 displays a set of Fe2*p* and Cr2*p* XPS spectra corresponding to as-received Fe_3O_4 samples prior and upon chemical cleaning. A detailed XPS line shape analysis reveals no significant differences between the Fe and Cr2*p* spectra in the two samples. The XPS peaks are mainly dominated by emissions from the characteristic oxidation states (Fe_3O_4, Cr_2O_3) (Andrés-Vergés et al. 2011; Chastain 1992). The integral peak areas after background subtraction and normalization using sensitivity factors provided by the electron energy analyser manufacturer were used to calculate the atomic concentration of each element. The chromium content results are displayed as a table in Fig. 6. There is a clear decrease in the Cr/Fe ratio and then in the Cr content upon the chemical cleaning of the sample. These values are equivalent to those obtained in the same samples upon mild Ar^+ ion bombardment to eliminate part of the carbon contamination present on their surfaces, which attenuates both the Fe and Cr emissions. These results demonstrate the partial regeneration of the adsorbent after NaOH treatment. The adsorption process involved two main steps. In the first step, physical adsorption of the Cr(VI) occurs, whereas in the second step, a chemical reaction takes place, reducing Cr(VI) and forming the Fe–Cr species that is strongly chemically adsorbed onto magnetite. Apparently, only the physisorbed Cr(VI) is eliminated by the NaOH treatment, while the chemically adsorbed Cr(VI) remains on the nanoparticle surface.

The reusability of the magnetite nanoparticles was investigated as a function of the diameter. After treatment with a NaOH solution and several washing steps, the nanoparticles were added to a fresh Cr(VI) solution at an initial concentration of 80 mg/L. Then, the magnetic nanoparticles were separated from the solution via a magnet, and the solution was examined to investigate the repeatability of the removal efficiency. Figure 5 depicts the recycle graph for different nanoparticle sizes. Remarkably, the nanoparticles maintained a distinguishable removal capability after five cycles for all of the investigated particle sizes, although a slight decrease was observed that was more significant for the smallest particles. As described above, the magnetization saturation of nanoparticles with a small diameter is considerably lower than that of nanoparticles with larger sizes, and thus, their separation from the solution via a magnet is more difficult, resulting in a partial loss of the nanoparticle adsorbent during the cycles.

Isotherms and kinetic adsorption

To further investigate the adsorption process of Cr(VI) on Fe_3O_4 nanoparticles, the Langmuir equation was employed (Eq. 1). The Langmuir isotherm is used when the adsorption phenomenon and the coverage behave as a monolayer with a finite number of adsorption sites (Gupta and Chen 1978). Once a site is filled, no further adsorption can occur at that site as long as the surface has reached a saturation point.

$$\frac{C_e}{Q_e} = \frac{1}{bQ_o} + \left(\frac{1}{Q_o}\right)C_e \quad (1)$$

where C_e is the equilibrium concentration of the adsorbate (mg/L), Q_e is the amount of adsorbate adsorbed per unit mass of adsorbent (mg/g), and b and Q_o are the Langmuir constants related to the monolayer adsorption capacity and the affinity of the adsorbent towards adsorbate, respectively.

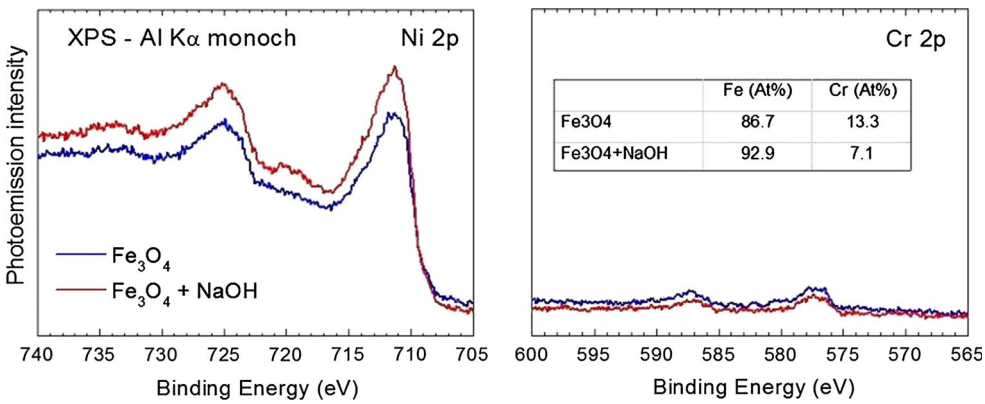

Fig. 6 Monochromatic Fe2*p* and Cr2*p* XPS spectra corresponding to (*blue line*) magnetic nanoparticles with a 21 nm diameter after the adsorption of Cr(VI) and (*red line*) after treatment for 2 h with 0.01 M NaOH. *Inset* compositional quantification in at.% concentration

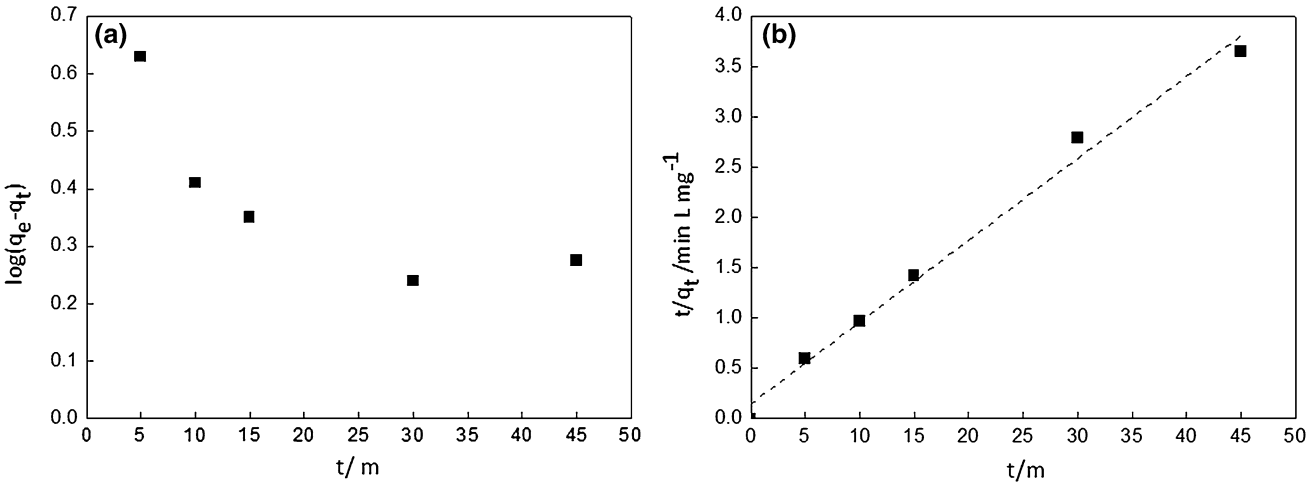

Fig. 7 Kinetic models for the adsorption of Cr(VI) onto magnetite nanoparticles with a 21 nm diameter at 20 °C and pH 3.5. **a** Pseudo-first-order model and **b** pseudo-second-order model

In this study, a linear dependence was observed in the graph of C_e/Q_e versus C_e, with a correlation coefficient $R^2 = 0.998$, indicating that the adsorption of Cr(VI) onto Fe_3O_4 nanoparticles follows a Langmuir isotherm. This fact corroborated that the process is governed by the adsorption of active sites on the surfaces, as when these active sites are saturated with Cr(VI), the nanoparticles are unable to remove more adsorbate.

The kinetics of Cr(VI) adsorption were evaluated using the pseudo-first-order and pseudo-second-order models, as shown in Fig. 7a, b, respectively. In the case of the pseudo-first-order kinetics, the equation used is as follows:

$$\log(q_e - q_t) = \log q_e - \frac{k_{ad} t}{2.303} \quad (2)$$

where k_{ad} is the pseudo-first-order rate constant (min^{-1}) of adsorption and q_e and q_t (mg/g) are the experimental adsorption capacity at equilibrium and the adsorption capacity at time t, respectively.

The pseudo-second order is defined by the following equation:

$$\frac{t}{q_t} = \frac{1}{k q_e^2} + \frac{t}{q_e} \quad (3)$$

where k is the pseudo-second-order rate constant of adsorption (g/mg min).

As can be observed, the pseudo-second-order equation fits this process well. Although at low Cr(VI) concentrations of <15 mg/L, a pseudo-first-order fitting model is suggested, as the Cr(VI) concentration increases, the fitting with the pseudo-first-order model declines. The pseudo-second-order kinetic model considers chemisorption to be the rate-limiting step, which occurs at high Cr(VI) concentrations and when the interactions of the ions and the active sites on the surface are effective. Yuan et al. (2009) previously studied the adsorption of Cr(VI) on magnetite nanoparticles and also on magnetite nanoparticles supported on montmorillonite, and they concluded that supported nanoparticles present much higher efficiency for the adsorption of Cr(VI). This was attributed to the fact that the magnetite nanoparticles are better dispersed when they are supported, which makes the synthetic approach more complex. In our work, the nanoparticles obtained by the electrochemical method are well dispersed in solution directly from synthesis, and they demonstrate high efficiency in removing Cr(VI) compared with other studies in which the nanoparticles were obtained by other strategies such as the coprecipitation method.

Conclusion

Well-dispersed magnetite NPs of various sizes were obtained by the electrochemical method, and their efficiency in removing Cr(VI) from aqueous solution was investigated. The adsorption of chromium was found to be highly dependent on parameters such as pH and temperature, with a great adsorption loading capability exhibited at pH values lower than 4 and at relatively high temperatures. Remarkably, it was demonstrated that the particle size of the NPs as well as their stability in aqueous solution has a strong influence on the chromium removal efficiency. The adsorption capacity progressively increases as the diameter decreases as a consequence of not only the higher surface area but also of their higher stabilization and lower aggregation. The magnetite NPs can be easily separated from the solution by applying an external magnetic field and reused as an adsorbent after removing the adsorbed Cr(VI) under alkaline conditions. Although the XPS measurements show that the number of active sites is not

completely recovered, the efficiency was largely maintained after five cycles. However, it was observed that the loss of this efficiency was more significant in the case of the smallest nanoparticles as a consequence of its low magnetization saturation value, which limits the manipulation of the NPs by a magnet and thereby their recovery. A further investigation of the adsorption process shows that the adsorption of Cr(VI) follows a Langmuir isotherm, with adsorption in a monolayer. In summary, the control of the different parameters affecting the removal of Cr(VI) from aqueous solution is crucial to achieve an adequate balance in recovery. In particular, the control of the particle size is of great importance for the applicability of these materials in wastewater, and in this regard, the electrochemical synthesis of magnetic NPs seems to be an appropriate and suitable strategy that allows for the preparation of relatively monodisperse NPs with good colloidal stability and for tuning the final diameter in a very simple manner.

Acknowledgments The authors are grateful to the Spanish Ministry of Science and Innovation (MAT2012-37109-C02-02, MAT2013-47878-C2-1-R and CSD2008-00023).

References

Aggarwal D, Goyal M, Bansal RC (1999) Adsorption of chromium by activated carbon from aqueous solution. Carbon 37:1989–1997. doi:10.1016/S0008-6223(99)00072-X

Andrés-Vergés M, Morales MP, Veintemillas-Verdaguer S, Palomares FJ, Serna CJ (2011) Core/shell magnetite/bismuth oxide nanocrystals with tunable size, colloidal, and magnetic properties. Chem Mater 24:319–324. doi:10.1021/cm202949q

Benefield LD, Judkins JF, Weand BL (1982) Process chemistry for water and wastewater treatment. Prentice-Hall, Englewood Cliffs

Boddu VM, Abburi K, Talbott JL, Smith ED (2003) Removal of hexavalent chromium from wastewater using a new composite chitosan biosorbent. Environ Sci Technol 37:4449–4456

Burks T et al (2014) Studies on the adsorption of chromium(VI) onto 3-mercaptopropionic acid coated superparamagnetic iron oxide nanoparticles. J Colloid Interface Sci 425:36–43. doi:10.1016/j.jcis.2014.03.025

Cabrera L, Gutierrez S, Menendez N, Morales MP, Herrasti P (2008) Magnetite nanoparticles: electrochemical synthesis and characterization. Electrochim Acta 53:3436–3441. doi:10.1016/j.electacta.2007.12.006

Chastain J, King RC, Moulder JF (1992) Handbook of X-ray photoelectron spectroscopy: a reference book of standard spectra for identification and interpretation of XPS data. [s.n.], Physical electronics. Eden Prairie, Perkin-Elmer

Chowdhury SR, Yanful EK, Pratt AR (2012) Chemical states in XPS and Raman analysis during removal of Cr(VI) from contaminated water by mixed maghemite–magnetite nanoparticles. J Hazard Mater 235–236:246–256. doi:10.1016/j.jhazmat.2012.07.054

Crane RA, Dickinson M, Popescu IC, Scott TB (2011) Magnetite and zero-valent iron nanoparticles for the remediation of uranium contaminated environmental water. Water Res 45:2931–2942

Dula T, Siraj K, Kitte SA (2014) Adsorption of hexavalent chromium from aqueous solution using chemically activated carbon prepared from locally available waste of bamboo (*Oxytenanthera abyssinica*). ISRN Environ Chem 2014:9. doi:10.1155/2014/438245

Faghihian H, Bowman RS (2005) Adsorption of chromate by clinoptilolite exchanged with various metal cations. Water Res 39:1099–1104. doi:10.1016/j.watres.2004.12.010

Gupta K, Chen K (1978) Arsenic removal by adsorption. J Water Pollut Control Fed 50:493

Hu J, Lo IMC, Chen G (2004) Removal of Cr(VI) by magnetite nanoparticle. Water Sci Technol 50:139–146

Hu J, Chen G, Lo I (2006) Selective removal of heavy metals from industrial wastewater using maghemite nanoparticle: performance and mechanisms. J Environ Eng 132:709–715. doi:10.1061/(ASCE)0733-9372(2006)132:7(709)

Hu J, Lo IMC, Chen G (2007) Comparative study of various magnetic nanoparticles for Cr(VI) removal. Sep Purif Technol 56:249–256

Khezami L, Capart R (2005) Removal of chromium(VI) from aqueous solution by activated carbons: kinetic and equilibrium studies. J Hazard Mater 123:223–231

Leyva Ramos R, Juarez Martinez A, Guerrero Coronado RM (1994) Adsorption of chromium(VI) from aqueous solutions on activated carbon. Water Sci Technol 30:191–197

Liu Y et al (2012) Synthesis of high saturation magnetization superparamagnetic Fe_3O_4 hollow microspheres for swift chromium removal. ACS Appl Mater Interfaces 4:4913–4920. doi:10.1021/am301239u

Mazario E, Morales MP, Galindo R, Herrasti P, Menendez N (2012) Influence of the temperature in the electrochemical synthesis of cobalt ferrites nanoparticles. J Alloys Compd 536(Supplement 1):S222–S225. doi:10.1016/j.jallcom.2011.10.073

Mor S, Ravindra K, Bishnoi NR (2007) Adsorption of chromium from aqueous solution by activated alumina and activated charcoal. Bioresour Technol 98:954–957. doi:10.1016/j.biortech.2006.03.018

Patterson RR, Fendorf S, Fendorf M (1997) Reduction of hexavalent chromium by amorphous iron sulfide. Environ Sci Technol 31:2039–2044. doi:10.1021/es960836v

Roisnel T, Rodriguez-Carvajal J (2000) WinPLOTR: a windows tool for powder diffraction patterns analysis. In: Materials science forum, proceedings of the seventh European powder diffraction conference (EPDIC 7), Barcelona (Spain), pp 118–123

Sanchez-Garcia JA et al (2009) Production of nanohole/nanodot patterns on Si(001) by ion beam sputtering with simultaneous metal incorporation. J Phys Condens Matter 21:0953–8984

Selvi K, Pattabhi S, Kadirvelu K (2001) Removal of Cr(VI) from aqueous solution by adsorption onto activated carbon. Bioresour Technol 80:87–89. doi:10.1016/S0960-8524(01)00068-2

Shahriari T, Nabi Bidhendi G, Mehrdadi N, Torabian A (2014) Effective parameters for the adsorption of chromium(III) onto iron oxide magnetic nanoparticle. Int J Environ Sci Technol 11:349–356. doi:10.1007/s13762-013-0315-z

Sharma YC, Srivastava V (2010) Comparative studies of removal of Cr(VI) and Ni(II) from aqueous solutions by magnetic nanoparticles. J Chem Eng Data 56:819–825. doi:10.1021/je100428z

Singh A, Prasad SM (2015) Remediation of heavy metal contaminated ecosystem: an overview on technology advancement. Int J Environ Sci Technol 12:353–366. doi:10.1007/s13762-014-0542-y

Singh DB, Gupta GS, Prasad G, Rupainwar DC (1993) The use of hematite for chromium(VI) removal. J Environ Sci Health Part A Environ Sci Eng Toxicol 28:1813–1826. doi:10.1080/10934529309375979

Vunain E, Mishra AK, Krause RW (2013) Fabrication, characterization and application of polymer nanocomposites for arsenic(III) removal from water. J Inorg Organomet Polym 23:293–305. doi:10.1007/s10904-012-9775-8

Yuan P et al (2009) Montmorillonite-supported magnetite nanoparticles for the removal of hexavalent chromium [Cr(VI)] from aqueous solutions. J Hazard Mater 166:821–829